JPET Fast Forward. Published on February 13, 2008 as DOI:10.1124/jpet.107.132357

JPET #132357

TITLE PAGE

α-AMINOAZAHETEROCYCLIC-METHYLGLYOXAL ADDUCTS DO NOT INHIBIT CFTR CHLORIDE CHANNEL ACTIVITY

N.D. Sonawane, Olga Zegarra-Moran, Wan Namkung, Luis J.V. Galietta and A.S. Verkman

Departments of Medicine and Physiology, University of California, San Francisco CA 94143-0521, (N.D.S., W.N., A.S.V.)

Laboratorio di Genetica Molecolare, Istituto Giannina Gaslini, 16148 Genova, Italy (O.Z.M., L.J.V.G.)

RUNNING TITLE PAGE

Running title: α-Aminoazaheterocyclic-methylglyoxals do not inhibit CFTR

Corresponding author: Alan S. Verkman, M.D., Ph.D., Departments of Medicine and Physiology, 1246 Health Sciences East Tower, University of California, San Francisco CA 94143-0521, U.S.A.

Phone: (415)-476-8530; Fax: (415)-665-3847; E-mail: Alan.Verkman@ucsf.edu

Number of text pages: 20

Number of tables: 0

Number of figures: 4

Number of references: 20

Number of words in Abstract: 178

Number of words in Introduction: 529

Number of words in Discussion: 669

Abbreviations: CFTR, cystic fibrosis transmembrane conductance regulator; CF, cystic fibrosis; $CFTR_{inh}$-172, 3-[(3-trifluoromethyl)phenyl]-5-[(4-carboxyphenyl)methylene]-2-thioxo-4-thiazolidinone; 3a,b, 2-amino-3-hydroxypyridine-methylglyoxal adducts; 4a,b, adenine-methylglyoxal adducts; 5a,b 2-deoxyadenosine-methylglyoxal adducts; 6a,b, adenosine-methylglyoxal adducts; 7a,b, 1-propylcytosine-methylglyoxal adducts; 8a,b, 1-aminoisoquinoline-methylglyoxal adducts; MalH-1, 2-naphthalenylamino-bis[(3,5-dibromo-2,4-dihydroxyphenyl)methylene]propanedioic acid dihydrazide; NMR, nuclear magnetic resonance; LC/MS, liquid chromatography/mass spectrometry; FRT, fisher rat thyroid; WT, wild-type; SPQ, 6-methoxy-*N*-(3-sulfopropyl)quinolinium; Forsk, forskolin

Recommended section assignment: Cellular and Molecular

ABSTRACT

Inhibitors of the cystic fibrosis transmembrane conductance regulator (CFTR) chloride channel have potential applications in the therapy of secretory diarrheas and polycystic kidney disease. Recently, several highly polar α-aminoazaheterocyclic-methylglyoxal adducts were reported to reversibly inhibit CFTR chloride channel activity with IC50 values in the low picomolar range (Routaboul et al. *J. Pharmacol. Exp. Ther.* 322:1023-1035), more than 10,000-fold better than that of thiazolidionone and glycine hydrazide CFTR inhibitors identified previously by high-throughout screening. Here, we resynthesized and evaluated the α-aminoazaheterocyclic-methylglyoxal adducts of Routaboul et al. reported to have high CFTR inhibition potency (compounds 5, 7 and 8). We verified that the reported synthesis procedures produced the target compounds in high yield. However, we found that these compounds did not inhibit CFTR chloride channel function in multiple cell lines at up to 100 μM concentration, using three independent assays of CFTR function including short-circuit current analysis, whole-cell patch-clamp and YFP-fluorescence quenching. As positive controls, near 100% CFTR inhibition was found by thiazolidionone and glycine hydrazide CFTR inhibitors. Our data provide direct evidence against CFTR inhibition by α-aminoazaheterocyclic-methylglyoxal adducts.

INTRODUCTION

The cystic fibrosis transmembrane conductance regulator (CFTR) protein is a cAMP-regulated chloride channel, which when mutated causes the hereditary disease cystic fibrosis (Sheppard and Welsh, 1999). CFTR in intestinal epithelial cells provides the primary route for chloride secretion in enterotoxin-mediated secretory diarrheas such as cholera and Traveler's diarrhea (Thiagarajah and Verkman, 2005). CFTR has also been implicated in the progressive expansion of renal cysts in polycystic kidney disease (Li et al., 2004; Yang et al., 2008). CFTR is thus a well-validated target for drug discovery (Verkman et al., 2006), with CFTR activators of potential utility in the therapy of cystic fibrosis, dry eye syndrome and constipation, and CFTR inhibitors in the therapy of secretory diarrheas and polycystic kidney disease. Our lab previously developed fluorescence, cell-based assays to identify CFTR activators (Galietta et al., 2001; Ma et al., 2002a) and inhibitors (Ma et al., 2002b; Muanprasat et al., 2004), and secondary electrophysiological and biochemical assays to verify their target and mechanism. Screening of ~200,000 synthetic small molecules yielded thiazolidinone and glycine hydrazide CFTR inhibitors with potencies down to ~0.2 μM (Ma et al., 2002b; Muanprasat et al., 2004). The glycine hydrazides block the CFTR pore at its external surface, which allowed the synthesis of non-absorbable polyethylene glycol and lectin adducts that do not cross membranes and block intestinal fluid secretion in animals models of cholera (Sonawane et al., 2006; 2007).

Routaboul et al. (2007) recently reported that α-aminoazaheterocyclic-methylglyoxal adducts inhibit CFTR chloride channel function completely and reversibly, with low picomolar IC_{50} values, more than 10,000-fold better than the most potent known CFTR inhibitors. The picomolar potency compounds were identified by screening a collection of seven α-aminoazaheterocyclic-methylglyoxal adducts. These adducts had been reported previously in a paper that described an efficient, one-step synthesis approach involving reaction of methylglyoxal with α-aminoaza-

heterocycles (Routaboul et al., 2002). The exceptionally high potency and reversibility of the α-aminoazaheterocyclic-methylglyoxals was surprising for several reasons. First, prior screening of 200,000 compounds for CFTR inhibition produced only one compound with an IC_{50} less than 1 μM, with an overall low verified hit rate of ~1/50,000 (Ma et al., 2002b; Muanprasat et al., 2004). Discovery of picomolar potency CFTR inhibitors from screening of seven compounds of a single chemical class is surprising, particularly because the compounds were tested for CFTR inhibition without a rational basis. Second, most channel inhibitors with picomolar potency are animal toxins rather than small, synthetic molecules (Benton et al. 2003; Castle et al 2003; Favreau et al., 2001; Grunnet et al., 2001). Last, contrary to the data of Routaboul et al. (2007), very slow (> hours) reversibility of picomolar-affinity inhibitors is expected even in the diffusion limit (Bkaily et al., 1985).

For these reasons and because of the potential major therapeutic implications of picomolar-potency CFTR inhibitors, we re-evaluated the findings of Routaboul et al. (2007). We verified the high-yield synthesis of α-aminoazaheterocyclic-methylglyoxal adducts, as originally reported by Routaboul et al. (2002); however, using multiple assays, cell lines and concentrations, and with appropriate positive controls, we were unable to demonstrate CFTR inhibition by the α-aminoazaheterocyclic-methylglyoxals.

METHODS

Synthesis procedures. ^{1}H-NMR spectra were obtained in D_2O (pH 7) using a 400 MHz Varian Spectrometer. Mass spectrometry was done on a Waters LC/MS system (Alliance HT 2790+ZQ, HPLC: Waters model 2690, Milford, MA). Flash chromatography was performed using EM silica gel (230-400 mesh), and thin layer chromatography on Merk silica gel 60 F254 plates.

Synthesis of α-aminoazaheterocycle-methylglyoxal adducts. Compounds 2, 3, 4, 5, 6, and 8 were synthesized in high yield following previously reported methods (Routaboul et al. 2002, 2007). Typically, a mixture of the aminoazaheterocycle and a dilute solution of methyl glyoxal were stirred under argon at ~50 ^{o}C for 1-2 days (until reaction complete by LC/MS). The residue after evaporation was purified by combination of precipitation, recrystallization, normal/reverse phase column chromatography, and preparative TLC (Routaboul et. al. 2002, 2007). Compound 7 was not synthesized due to commercial unavailability of starting materials. Original NMR and MS data are included in Supplemental Information.

2-Amino-pyridine adducts 2ab: Yield, 76%; ^{1}H NMR: 8.15-7.88 (1H, m, Ar-H), 7.76-7.48 (1H, m, Ar-H), 6.82-6.80 (1H, d, Ar-H), 6.78-6.715 (1H, t, Ar-H), 4.30/3.93 (1H, s, CH), 1.50 (3H, s, CH_3), 1.39 (3H, s, CH_3); MS (ES^+) (*m/z*): 239 $[M+1]^+$.

2-Amino-3-hydroxypyridine adducts 3ab: Yield: 76%; m.p.: 141-142 ^{o}C (decomposition); ^{1}H-NMR: 7.31-7.21 (1H, m, CH), 6.64-6.52 (2H, m, CH), 4.30/3.89 (1H, s, m, CH), 1.52-1.42 (3H, bs, CH_3), 1.38 (3H, s, CH_3); MS (ES^+) (*m/z*): 255 $[M+1]^+$.

Adenine adducts 4ab: Yield, 66%; ^{1}H-NMR: 8.29 (1H, s, CH); 8.01 (1H, s, CH); 4. 69 (1H, s, CH); 1.86/1.47 (3H, s, CH_3); MS (ES^+) (*m/z*): 280 $[M+1]^+$.

Deoxy-adeninosine adducts 5ab: Yield: 67%; ^{1}H-NMR:; 8.23 (s, 1H, Ar-CH), 8.16 (d, 1H, Ar-CH), 6.30 (t, 1H, N-CH), 4.79 (d, 1H, adduct CH), 4.50-4.44 (m, 1H, CH), 4.01 (q, 1H, CH), 3.68-3.58 (2 dd or q, 2H, DO-CH_2), 2.70-2.63 (m, 1H, CH_2), 2.42-2.36 (m, 1H, CH_2), 1.93 (s, 3H, CH_3), 1.46 (s, 3H, CH_3); MS (ES^+) (*m/z*): 396 $[M+1]^+$.

Adenosine adducts 6ab: Yield, 59%; ^{1}H-NMR: 8.32 (s, 1H, Ar-H), 8.18 (s, 1H, Ar-H), 5.89 (d, 1H, N-CH), 5.10/4.74 (s, 1H, adduct CH), 4.34 (t, 1H, CH), 4.09 (q, 1H, CH), 4.01 (q, 1H, CH_2), 3.76-3.62 (2 dd or q, 2H), 3.45/3.36 (q, 2H), 2.15 (s, 3H, CH_3), 1.86 (s, 3H, CH_3); MS (ES^+) (*m/z*): 412 $[M+1]^+$.

1-Aminoisoquinoline adducts 8ab: Yield, 71%; m.p. 175-177 ^{o}C (decomposition); ^{1}H NMR: 8.31-8.21 (1H, m, Ar-H), 7.86-7.47 (4H, m, Ar-H) 7.14-6.99 (1H, m, Ar-H), 4.37 & 4.05 (1H, s, CH), 1.64 (3H, s, CH_3), 1.57 (3H, s, CH_3); MS (ES^+) (*m z*): 289 $[M+1]^+$.

Fluorescence cell-based assay of CFTR inhibition. FRT cells stably co-transfected with human wildtype CFTR and YFP-H148Q, as described (Ma et al., 2002a), were plated in black-walled, 96-well plates with transparent plastic bottom (Corning-Costar), cultured overnight to confluence, washed three times with PBS, and incubated with test compounds in a final volume of 60 µl. YFP-H148Q fluorescence was measured using a fluorescence plate-reader (FluoStar Optima; BMG Lab Technologies) equipped with custom excitation and emission filters (500 nm and 544 nm, respectively, Chroma). Fluorescence intensity in each well was measured for a total of 14 seconds. In each well 100 µl of PBS/I^- (PBS with 100 mM Cl^- replaced by I^-) was injected by a syringe pump at two seconds after the start of data collection. The initial rate of fluorescence decay caused by I^- influx was measured to determine CFTR activity (Ma et al., 2002a).

Short-circuit current measurements. FRT cells (stably expressing human wildtype CFTR) were cultured on Snapwell filters with 1 cm^2 surface area (Corning-Costar) to resistance >1,000 $\Omega \cdot cm^2$, as described (Ma et al., 2002a). Filters were mounted in an Easymount Chamber System (Physiologic Instruments, San Diego). For apical Cl^- current measurements the basolateral hemichamber

contained (in mM): 130 NaCl, 2.7 KCl, 1.5 KH_2PO_4, 1 $CaCl_2$, 0.5 $MgCl_2$, 10 Na-HEPES, 10 glucose (pH 7.3). The basolateral membrane was permeabilized with amphotericin B (250 µg/ml) for 30 min. In the apical solution 65 mM NaCl was replaced by sodium gluconate, and $CaCl_2$ was increased to 2 mM. Solutions were bubbled with 95% O_2/ 5% CO_2 and maintained at 37 ºC. Current was recorded using a DVC-1000 voltage-clamp (World Precision Instruments) using Ag/AgCl electrodes and 1 M KCl agar bridges. Some measurements were done using T84 colonic epithelial cells and primary cultures of human bronchial epithelial cells, which natively express human wildtype CFTR), as described previously (Galietta et al., 2000). Short-circuit current was also measured in freshly isolated mouse ileum using symmetric bicarbonate-containing solutions, as described previously (Thiagarajah et al., 2004).

Whole-cell patch-clamp. Patch-clamp experiments were carried out at room temperature on FRT cells stably expressing human wildtype CFTR, as described (Taddei et al., 2004). Some experiments were done using CHO cells after transient transfection with human wildtype CFTR. Briefly, the pipette solution contained (in mM): 120 CsCl, 10 TEA-Cl, 0.5 EGTA, 1 $MgCl_2$, 40 mannitol, 10 Cs-HEPES (pH 7.3), 1 mM MgATP, and 0.4 µg/ml of catalytic subunit of protein kinase A. The bath solution contained (in mM): 150 NaCl, 1 $CaCl_2$, 1 $MgCl_2$, 10 glucose, 10 mannitol, 10 Na-Hepes (pH 7.4). The cell membrane was clamped at specified voltages using an EPC-7 patch-clamp amplifier (List Medical). Voltage stimulation consisted in alternate pulses to -100 and +100 mV from a holding potential of 0 mV. Where needed, a full range of voltage pulses was applied in 20 mV steps, with pulse duration 800 ms. Data were filtered at 500 Hz and digitized at 1000 Hz using an Instrutech ITC-16 AD/DA interface and the PULSE (Heka) software. Inhibitors were applied by extracellular perfusion.

Transient transfection of CHO cells. CHO cells, plated in 6-well plates (500,000 cells/well) were transfected with 4 µg of plasmid DNA and 10 µl of Lipofectamine 2000 (Invitrogen) per well following manufacturer's instructions. Cells were cotransfected with two plasmids carrying the coding sequence for CFTR and for the yellow fluorescent protein, in a 3:1 molar ratio. After 24 hours, cells were detached by trypsinization and sorted with a FACS. Fluorescent cells were isolated and plated in 35 mm Petri dishes for whole-cell patch-clamp recordings.

RESULTS

*Synthesis and characterization of α-*aminoazaheterocyclic-methylglyoxal *adducts*

Fig. 1A shows chemical structures of the two CFTR inhibitors, $CFTR_{inh}$-172 and MalH-1, identified previously by high-throughput screening. Fig. 1B shows the α-aminoazaheterocyclic-methylglyoxal adducts reported by Routaboul et al. (2007) to strongly inhibit CFTR with IC_{50} values in the low picomolar to nanomolar range. All adducts were mixture of at least two diastereomers, in approximately 50:50 proportion, and were highly soluble in water, except for 8ab, which had low solubility. By preparative TLC and column chromatography, we were successful in separating diastereomers 3ab but not 5ab. Routaboul et al. (2007) tested all adducts as diastereomeric mixtures except the adduct 5a. Because we found that mixture 5ab was inactive at concentrations to 10^6-fold greater than the reported IC_{50} by Routaboul et al. (2007), we did not work further in separating 5a and 5b.

Fig. 1C shows the chemical reaction scheme reported by Routaboul et al. (2002) for efficient, one-step synthesis of α-aminoazaheterocyclic-methylglyoxals. The reported reaction conditions and workup procedures gave the target adducts with yields > 50%. The reactions were monitored by TLC and LC/MS, with completion of reaction indicated by absence of the α-aminoazaherocycle. In most cases the purified material showed two clear peaks with corresponding molecular weights of

adducts, indicating presence of diastereomers (see Supplementary Information). NMR spectra of all adduct showed the presence of two peaks corresponding to methyl protons and two peaks corresponding to ring C-H protons. Our ^{1}H-NMR spectra of 3ab and 8ab were in agreement with previously reported spectra in Routaboul et al. (2007). We also report here the NMR data for 2ab, 4ab, 5ab and 6ab (see Supplementary Information), which were not included in Routaboul et al. (2002).

CFTR inhibition measurements

Measurements of CFTR inhibition were done first using FRT cells expressing human wildtype CFTR, an established cell line that was used for primary high-throughput screening to identify inhibitors and activators of wildtype CFTR (Ma et al., 2002ab; Muanprasat et al., 2004), and for secondary electrophysiological assays (Taddei et al., 2004). This cell line expresses CFTR strongly and contains no other cAMP-regulated anion current. Figs. 2A shows representative short-circuit current measurements, in which apical membrane current (I_{ap}) provides a direct measure of CFTR chloride conductance. Apical membrane current rapidly increased following addition of the cell-permeable cAMP agonist forskolin. However, compounds 3ab 4ab, 5ab and 8ab did not demonstrably reduce apical membrane current, which was rapidly reduced to approximately zero following addition of the CFTR inhibitor MalH-1 at the end of each measurement. Similar lack of CFTR inhibition was found for compounds 2ab and 6ab (data not shown). In control experiments, apical membrane current was reduced in a concentration-dependent manner by the CFTR inhibitors, $CFTR_{inh}$-172 (Fig. 2B) and MalH-1 (not shown), with near 100% inhibition seen at higher concentrations (Ma et al., 2002b; Sonawane et al, 2006).

We also tested all compounds in a fluorescence-based plate reader assay in which CFTR function is assayed from the rate of iodide influx (negative slope) in FRT cells co-expressing human

wildtype CFTR and the cytoplasmic iodide sensor YFP-H148Q (Ma et al., 2002b). In this assay, CFTR inhibition reduces iodide influx and thus decreases the rate of quenching of GFP fluorescence (negative slope). Fig. 2C shows concentration-inhibition data for the known CFTR inhibitor MalH-DIDS (Sonawane et al., 2007), along with the 5ab and 8ab α-aminoazaheterocyclic-methylglyoxals, neither of which measurably inhibited CFTR at any concentration tested. Similar lack of CFTR inhibition was found for compounds 3ab and 4ab (not shown).

Short-circuit current measurements were also done on two cell types that natively express human wildtype CFTR, T84 colonic epithelial cells and primary cultures of human bronchial epithelial cells, as well as in mouse intestine. Fig. 3 shows short-circuit current data for active chloride secretion, in which measurements were done in non-permeabilized cells in the absence of a chloride gradient. As above, increased current corresponds to apical membrane CFTR chloride conductance. Forskolin produced a prompt increase in chloride current as a result CFTR activation in T84 cells. Each of the α-aminoazaheterocyclic-methylglyoxals tested did not reduce chloride current (Fig. 3A). In each case the CFTR inhibitor $CFTR_{inh}$-172 reduced current to near-zero at the end of the experiment. Similar lack of inhibition was found in human bronchial epithelial cells for compound 8ab (Fig. 3B). Also, the α-aminoazaheterocyclic-methylglyoxals at high concentration did not inhibit short-circuit in mouse ileal epithelium (Fig. 3C).

Whole-cell patch-clamp recordings in FRT cells were obtained as another independent, direct measure of CFTR chloride channel function. Representative data for compound 5ab is provided. Fig. 4A shows whole-cell membrane current in response to voltage pulses at -100 mV (filled symbols) and +100 mV (open symbols) from a holding potential of 0 mV. Where indicated by letters (a-f), the alternate voltage stimulation was interrupted to apply voltage pulses in the range -100 to +100 mV in 20 mV steps. The resulting current-voltage relationships and membrane currents are shown in Fig. 4B and 4C, respectively. Membrane currents were very small at baseline,

but increased strongly upon stimulation with CPT-cAMP (100 μM). The voltage relationship of cAMP-activated currents was linear (Fig. 4B), as expected for CFTR-dependent activity. Subsequent addition of compound 5ab (100 μM) did not affect membrane currents at all membrane potentials (Fig. 4A-C), whereas $CFTR_{inh}$-172 (10 μM) reduced CFTR current to near-zero. Similar whole-cell patch-clamp analysis for compounds 5ab and 8ab, in the concentration range 100 nM – 100 μM, showed no significant CFTR inhibition. Looking further for a possible explanation for our conflicting results, we repeated the whole-cell patch-clamp recordings on CFTR-expressing CHO cells, the cell type used by Routaboul et al. (2007). Fig. 4D shows that, similar to FRT cells, no inhibition was found for compound 5ab at high concentration.

Together, the short-circuit current, fluorescence and patch-clamp analyses provide direct evidence against CFTR inhibition by α-aminoazaheterocyclic-methylglyoxal adducts.

DISCUSSION

The goal of our study was to evaluate the CFTR inhibition potency of the α-aminoaza-heterocyclic-methylglyoxal adducts reported by Routaboul et al. (2007). This investigation was motivated by the potential utility of potent small-molecule CFTR inhibitors in the therapy of secretory diarrheas and polycystic kidney disease. Based on the much greater reported potency of the α-aminoazaheterocyclic-methylglyoxals than known CFTR inhibitors, verification of their potency and mechanism-of-action is important in selecting compound classes for clinical development. Though our experiments reproduced the synthesis procedures and analytical data of several α-aminoazaheterocyclic-methylglyoxals, we were unable to demonstrate CFTR inhibition using multiple cell lines and several established assay methods, with experiments done in two independent laboratories in San Francisco, USA and Genoa, Italy. In each case positive controls with known CFTR inhibitors validated the sensitivity of the assays. As mentioned in the

Introduction, for a number of reasons it was quite surprising *a priori* that CFTR inhibitors with low picomolar potency could be discovered after screening of a very small set of compounds of a single chemical class. These compounds had been synthesized previously as examples of a novel, one-step stereoselective reaction of methylglyoxal with α-aminoazaheterocycle (Routaboul et al., 2002).

We cannot account for the CFTR inhibition potency data reported by Routaboul et al. (2007). The simple, one-step synthesis, done exactly as reported by Routaboul et al. (2002), yielded the compounds in high yield. Analytical data for the compounds reported by Routaboul et al. (2002) and those synthesized here were in agreement. Mass spectra showed correct molecular weights indicating the adduct formation from two methylglyoxal molecules with one α-aminoazaheterocycle.

With regard to the CFTR inhibition studies reported by Routaboul et al. (2007), there appear to be technical concerns and inconsistencies. Our whole-cell patch clamp recordings show that lack of inhibition in short-circuit current and fluorescence experiments could not be due to an unusual voltage-dependence of α-aminoazaheterocyclic-methylglyoxals. We found no significant inhibition at all applied voltages in the -100 to +100 mV range, the same used by Routaboul et al. (2007). We also tested concentrations up to 10^6-fold higher than the reported IC_{50}, making it unlikely that lack of inhibition is due to insufficient concentration or membrane permeability. Our whole-cell patch-clamp results in FRT and CHO cells do not agree with those of Routaboul et al. (2007) in which 10 pM, a concentration that is ten times lower than the IC50 reported by the same authors, fully blocked CFTR currents. The SPQ fluorescence measurements (Fig. 7 of Routaboul et al., 2007) appear as well to be internally inconsistent, as inhibition was determined from the initial upslope of the curves in the first few seconds just after nitrate addition in the presence of inhibitor. Finding of inhibition at this early time is inconsistent with their data in Fig. 4, panel C showing ~1 min kinetics for onset of inhibition. We also note that such a rapid onset of inhibition is inconsistent with the high polarity and solubility of the α-aminoazaheterocyclic-methylglyoxals, as their permeation across cell plasma

membrane to bind to an inhibition site in the cell interior should be very slow. An interior binding site is mandated by the data in Fig. 8 of Routaboul et al. (2007), showing remarkably weaker CFTR inhibition after mutation (G551D) at a residue located in a cytosolic domain of CFTR. Finally, the intestinal short-circuit current measurements in Fig. 10 of Routaboul et al. (2007) appear to be flawed in that inhibitors were added prior to rather than after forskolin simulation of CFTR. Whereas an appropriate forskolin response was seen in panel A of their Fig. 10, the near-zero baseline current in the intestinal strips studied in panels B and C, prior to inhibitor addition, suggests non-viable tissue. The reduced forskolin response in these panels is thus a consequence of poor tissue viability rather than CFTR inhibition. We found no inhibition of CFTR-dependent short-circuit current in mouse intestine by the α-aminoazaheterocyclic-methylglyoxals.

In conclusion, the α-aminoazaheterocyclic-methylglyoxal adducts reported by Routaboul et al. (2007) lack CFTR inhibition activity and are thus not candidates for further development.

REFERENCES

Benton DC, Monaghan AS, Hosseini R, Bahia PK, Haylett DG and Moss GW (2003) Small conductance Ca^{2+}-activated K^+ channels formed by the expression of rat SK1 and SK2 genes in HEK 293 cells. *J Physiol* **553:**13-19.

Bkaily G, Sperelakis N, Renaud JF and Payet MD (1985) Apamin, a highly specific Ca^{2+} blocking agent in heart muscle. *Am J Physiol* **248:**H961-H965.

Castle NA, London DO, Creech C, Fajloun Z, Stocker JW and Sabatier JM (2003) Maurotoxin: a potent inhibitor of intermediate conductance Ca^{2+}-activated potassium channels. *Mol Pharmacol* **63:**409-418.

Favreau P, Gilles N, Lamthanh H, Bournaud R, Shimahara T, Bouet F, Laboute P, Letourneux Y, Menez A, Molgo J and Le Gall F (2001) A new omega-conotoxin that targets N-type voltage-sensitive calcium channels with unusual specificity. *Biochemistry* **40:**14567-14575.

Galietta LJ, Folli C, Marchetti C, Romano L, Carpani D, Conese M and Zegarra-Moran O (2000) Modification of transepithelial ion transport in human cultured bronchial epithelial cells by interferon-gamma. *Am J Physiol* **278:**L1186-L1194

Galietta LJ, Springsteel MF, Eda M, Niedzinski EJ, By K, Haddadin MJ, Kurth MJ, Nantz MH and Verkman AS (2001) Novel CFTR chloride channel activators identified by screening of combinatorial libraries based on flavone and benzoquinolizinium lead compounds. *J Biol Chem* **276:**19723-19728.

Grunnet M, Jensen BS, Olesen SP and Klaerke DA (2001) Apamin interacts with all subtypes of cloned small-conductance Ca^{2+}-activated K^+ channels. *Pflugers Arch* **441:**544-550.

Kunzelmann K and Mall M (2002) Electrolyte transport in the mammalian colon: mechanisms and implications for disease. *Physiol Rev* **82:**245-289.

Li H, Findlay IA and Sheppard DN (2004) The relationship between cell proliferation, Cl^- secretion, and renal cyst growth: a study using CFTR inhibitors. *Kidney Int* **66**:1926-1938.

Ma T, Vetrivel L, Yang H, Pedemonte N, Zegarra-Moran N, Galietta, LJV and Verkman AS (2002a) High-affinity activators of CFTR chloride conductance identified by high-throughput screening. *J Biol Chem* **277**:37235-37241.

Ma T, Thiagarajah JR, Yang H, Sonawane ND, Folli C, Galietta LJ and Verkman AS (2002b) Thiazolidinone CFTR inhibitor identified by high-throughput screening blocks cholera toxin-induced intestinal fluid secretion. *J Clin Invest* **110:**1651-1658.

Muanprasat C, Sonawane ND, Salinas D, Taddei A, Galietta LJ and Verkman AS (2004) Discovery of glycine hydrazide pore-occluding CFTR inhibitors: mechanism, structure-activity analysis, and in vivo efficacy. *J Gen Physiol* **124:**125-137.

Routaboul C, Dumas L, Vergne J, Gautier-Luneau I, Maurel M-C and Décout J-L (2002) New stereoselective reaction of methylglyoxal with 2-aminopyridine and adenine derivatives: formation of imino acid-nucleic base derivatives in water under mild conditions. *Chem Commun* **10:**1114–1115.

Routaboul C, Norez C, Melin P, Molina MC, Boucherle B, Bossard F, Noel S, Robert R, Gauthier C, Becq F and Decout JL (2007) Discovery of α-aminoazaheterocycle-methylglyoxal adducts as a new class of high-affinity inhibitors of cystic fibrosis transmembrane conductance Regulator chloride channels. *J Pharmacol Exp Ther* **322:**1023-1035.

Sheppard DN and Welsh MJ (1999) Structure and function of the CFTR chloride channel. *Physiol Rev* **79:**S23-S45.

Sonawane ND, Hu J, Muanprasat C and Verkman AS (2006) Luminally-active, nonabsorbable CFTR inhibitors as potential therapy to reduce intestinal fluid losses in cholera. *FASEB J* **20**:130-132.

Sonawane ND, Zhao D, Zegarra-Mora O, Galietta LJV and Verkman AS (2007) Lectin conjugates as potent, nonabsorbable CFTR inhibitors for reducing intestinal fluid secretion in cholera. *Gastroenterology* **132**:1234-1244.

Taddei A, Folli C, Zegarra-Moran O, Fanen P, Verkman AS and Galietta LJ (2004) Altered channel gating mechanism for CFTR inhibition by a high-affinity thiazolidinone blocker. *FEBS Lett* **558:**52-56.

Thiagarajah J, Broadbent T, Hsieh E and Verkman AS (2004). Prevention of toxin-induced intestinal ion and fluid secretion by a small-molecule CFTR inhibitor. *Gastroenterology* **126**:511-519.

Thiagarajah JR and Verkman AS. (2005) New drug targets for cholera therapy. *Trends Pharmacol Sci* **26:**172-175.

Verkman AS, Lukacs GL and Galietta LJ (2006) CFTR chloride channel drug discovery - inhibitors as antidiarrheals and activators for therapy of cystic fibrosis. *Curr Pharm Des* 12:2235-2247.

Yang B, Sonawane, ND, Zhao, D, Somlo, S and Verkman AS (2008). Small-molecule CFTR inhibitors slow cyst growth in culture and mouse models of polycystic kidney disease. *J Am Soc Nephrol* In press.

FOOTNOTES

Supported by grants DK72517, HL73854, EB00415, EY13574, DK35124 and DK43840 from the National Institutes of Health, and Drug Discovery and Research Development Program grants from the Cystic Fibrosis Foundation.

Reprint requests to: Alan S. Verkman, M.D., Ph.D., Departments of Medicine and Physiology, 1246 Health Sciences East Tower, University of California, San Francisco CA 94143-0521, U.S.A. Phone: (415)-476-8530; Fax: (415)-665-3847; E-mail: Alan.Verkman@ucsf.edu

LEGENDS FOR FIGURES

Figure 1. **Structures and synthesis of α-aminoazaheterocyclic-methylglyoxal adducts.** *A,* Structures of thiazolidinone CFTR inhibitor $CFTR_{inh}$-172 and malonic acid hydrazide CFTR inhibitor MalH-1. *B,* Structures of α-aminoazaheterocyclic-methylglyoxals (from Routaboul et al., 2007) reported to inhibit CFTR. *C,* Reaction scheme for synthesis of α-aminoazaheterocyclic-methylglyoxals adducts. Aqueous mixture of starting materials stirred at ~50 ^{o}C until disappearance of α-aminoheterocycle.

Figure 2. **CFTR inhibition studies in FRT cells expressing human wildtype CFTR.** *A,* Short-circuit current analysis, showing apical membrane current in permeabilized FRT cells in the presence of a transepithelial chloride gradient. Responses shown to cAMP agonist forskolin (20 μM), followed by indicated concentrations of test compounds. Each experiment representative of 3-5 measurements on separate cell cultures. *B,* Control study using CFTR inhibitor $CFTR_{inh}$-172. *C,* Concentration-inhibition data from YFP fluorescence quenching plate reader assay.

Figure 3. **Short-circuit analysis of epithelial cells that natively express wildtype CFTR: T84 colonic cells, primary cultures of human bronchial cells, and mouse intestine.** *A,* Short-circuit current in non-permeabilized T84 cells in the absence of a chloride gradient. Responses shown to forskolin (20 μM) followed by indicated concentrations of test compounds. *B,* Short-circuit current recording from human bronchial epithelial cells. C, Compound effects on short-circuit current in mouse ileum. CFTR chloride current stimulated by forskolin (20 μM) and isobutylmethylxanthine (100 μM). Compounds tested at 10 μM (S.E., n=3). Percentage inhibition by 5ab and 8ab not significantly different from zero.

Figure 4. **Whole-cell patch-clamp study of CFTR inhibition.** *A*, Time course of whole-cell membrane currents elicited at +100 (open symbols) and -100 mV (filled symbols) in a CFTR-expressing FRT cell. Where indicated, cells were stimulated with 100 µM CPT-cAMP and challenged with 5ab (100 µM) and $CFTR_{inh}$-172 (10 µM). Where indicated by lower case letters, the alternate stimulation was interrupted to apply scaled voltage steps. *B*, Current-voltage relationships generated from the experiment in A (baseline current subtracted). *C*, Superimposed membrane currents induced at different membrane potentials (from –100 to +100 mV) in 20 mV steps (from the same experiment). *D*, Membrane currents from CHO cells expressing CFTR. The first three panels show superimposed membrane currents induced at different membrane potentials with 100 µM CPT-cAMP alone or in combination with 5ab (100 µM) or $CFTR_{inh}$-172 (10 µM). The fourth panel shows the corresponding current-voltage relationship (one set of experiments typical of three).

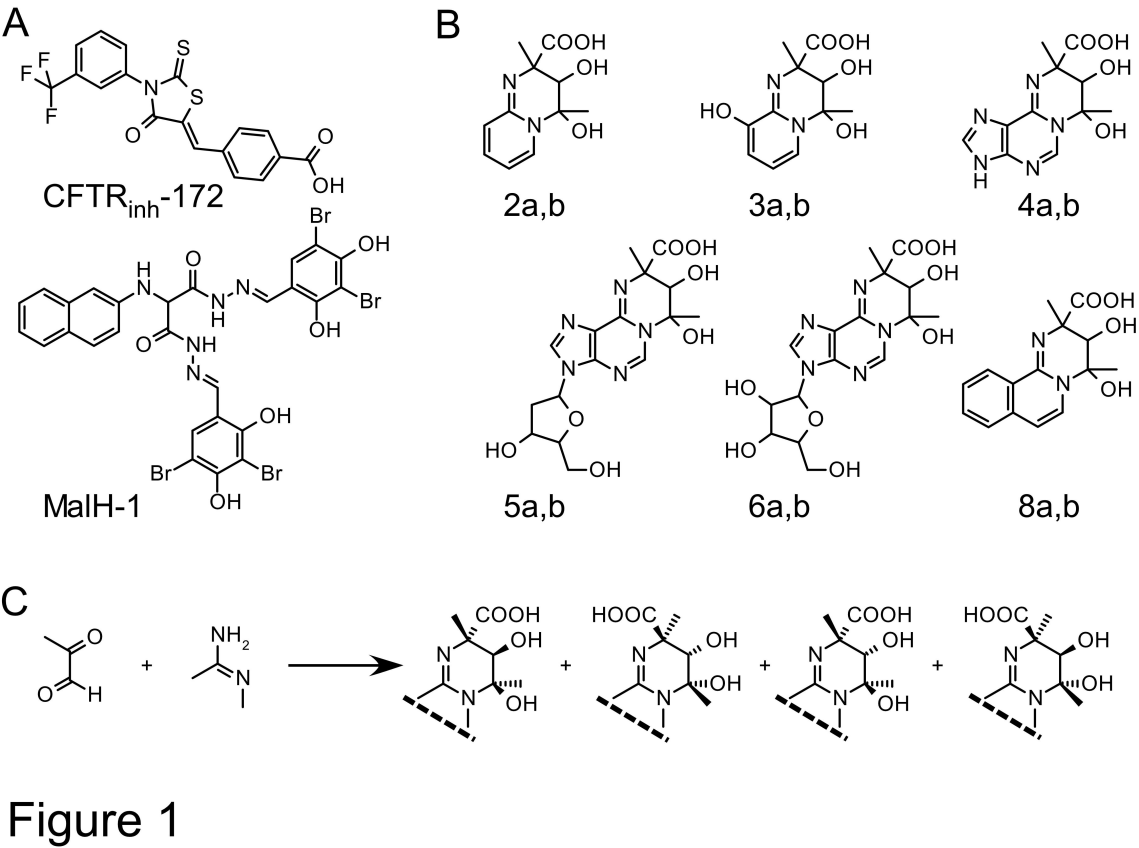

Figure 1

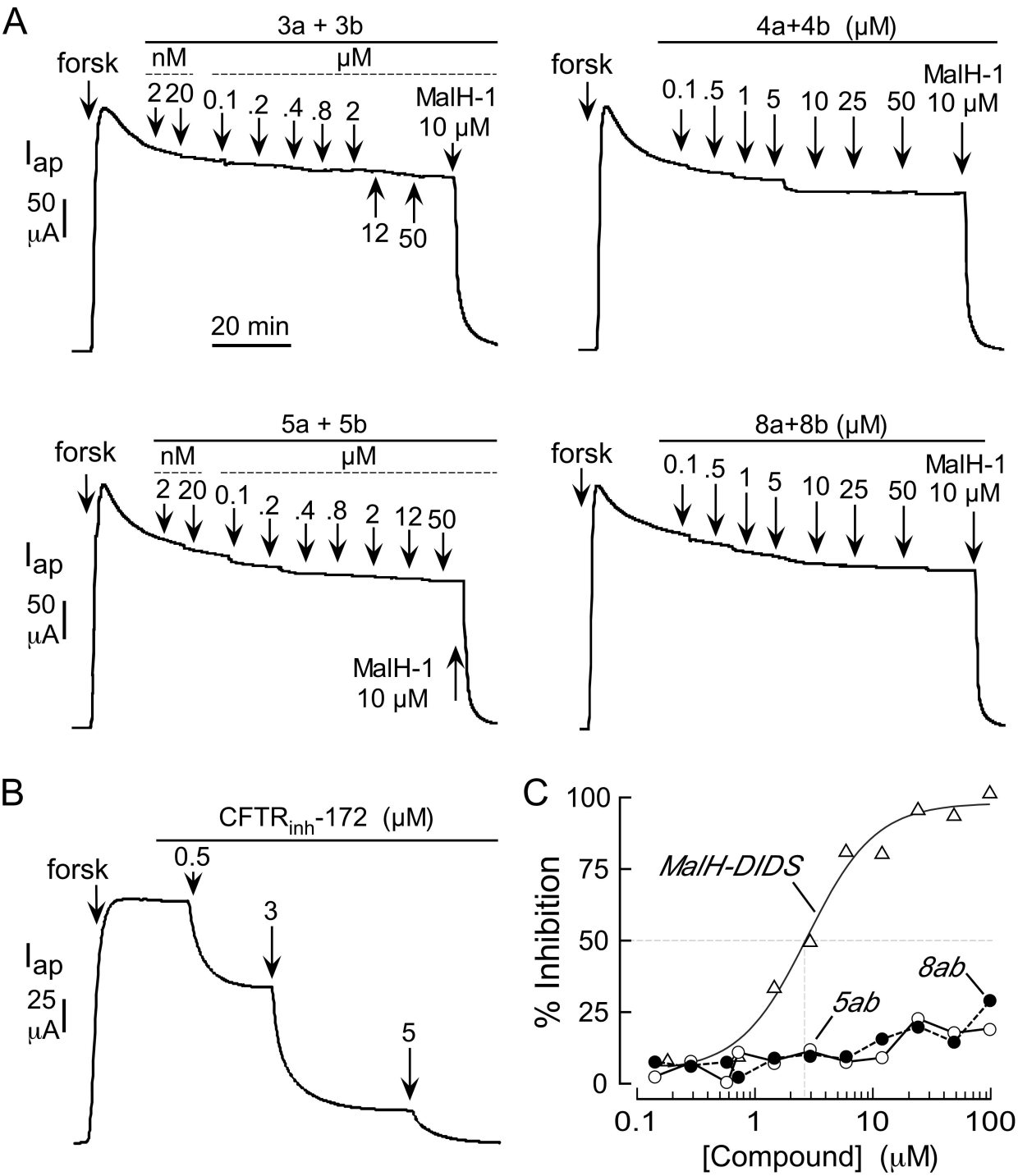
A
3a + 3b
forsk
nM
μM
2 20 0.1 .2 .4 .8 2
MalH-1
10 μM
I_{ap}
50
μA
12 50
20 min
4a+4b (μM)
forsk
0.1 .5 1 5 10 25 50
MalH-1
10 μM
5a + 5b
forsk
nM
μM
2 20 0.1 .2 .4 .8 2 12 50
I_{ap}
50
μA
MalH-1
10 μM
8a+8b (μM)
forsk
0.1 .5 1 5 10 25 50
MalH-1
10 μM
B
$CFTR_{inh}$-172 (μM)
forsk
0.5
3
5
I_{ap}
25
μA
C
% Inhibition
100
75
50
25
0
MalH-DIDS
8ab
5ab
0.1
1
10
100
[Compound] (μM)

Figure 2

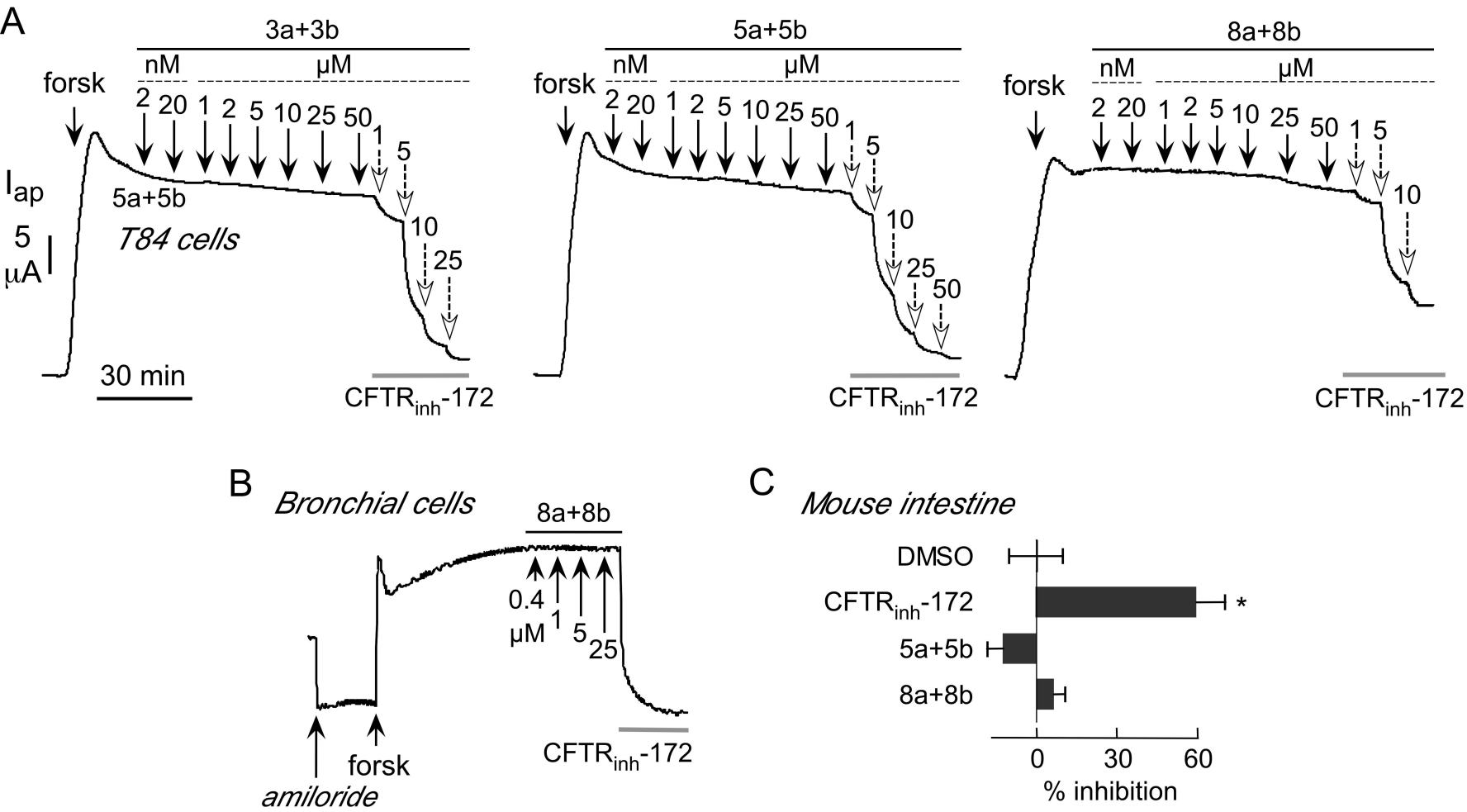
A
3a+3b
nM
µM
forsk
2 20 1 2 5 10 25 50 1 5
5a+5b
10
25
I_{ap}
5 µA
T84 cells
30 min
$CFTR_{inh}$-172
5a+5b
nM
µM
forsk
2 20 1 2 5 10 25 50 1 5
10
25 50
$CFTR_{inh}$-172
8a+8b
nM
µM
forsk
2 20 1 2 5 10 25 50 1 5
10
$CFTR_{inh}$-172
B
Bronchial cells
8a+8b
0.4 µM 1 5 25
forsk
amiloride
$CFTR_{inh}$-172
C
Mouse intestine
DMSO
$CFTR_{inh}$-172
5a+5b
8a+8b
*
0 30 60
% inhibition

Figure 3

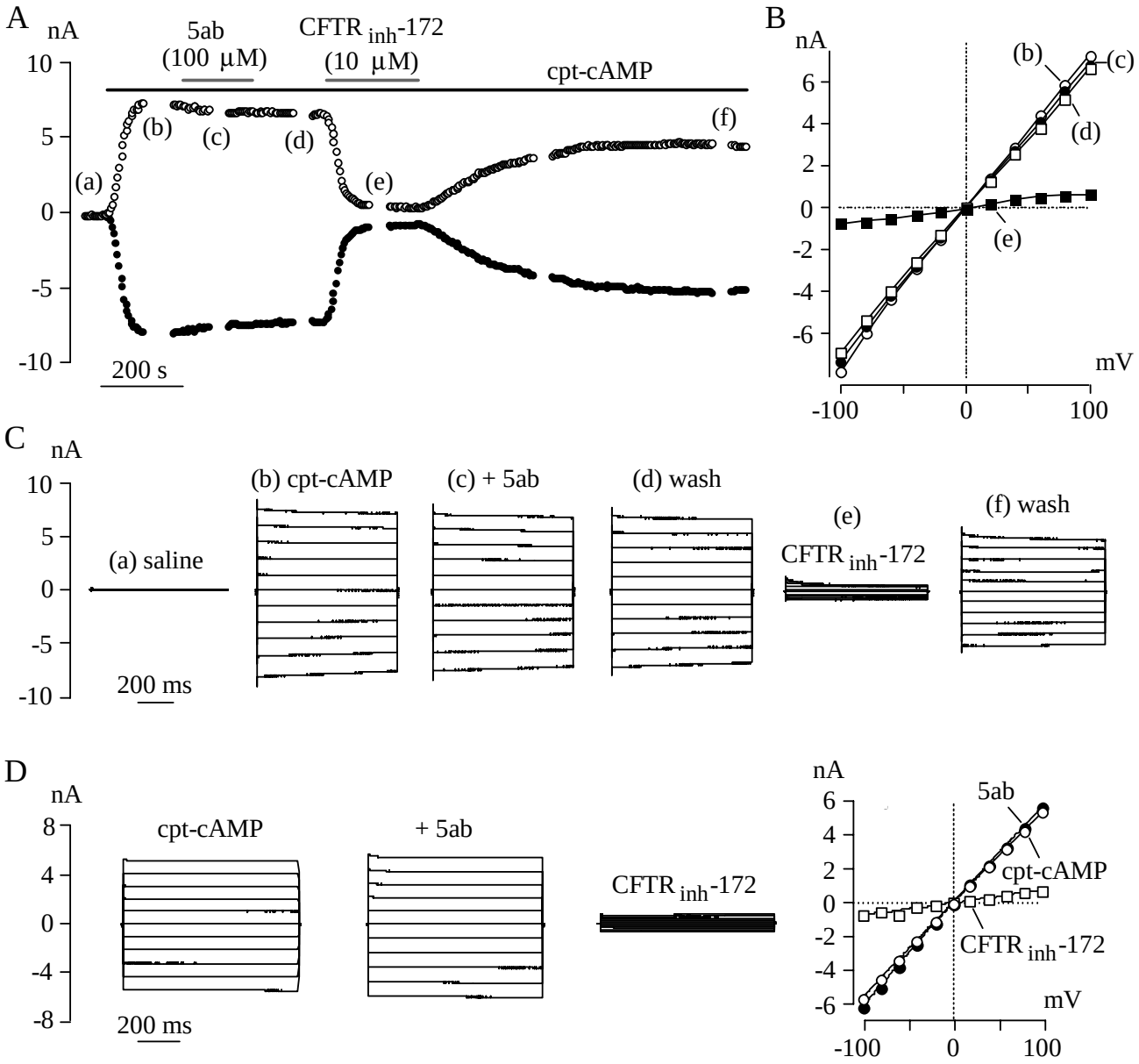
A
nA
5ab
(100 µM)
CFTR inh-172
(10 µM)
cpt-cAMP
10
5
0
-5
-10
(a)
(b)
(c)
(d)
(e)
(f)
200 s
B
nA
6
4
2
0
-2
-4
-6
(b)
(c)
(d)
(e)
mV
-100
0
100
C
nA
10
5
0
-5
-10
(a) saline
(b) cpt-cAMP
(c) + 5ab
(d) wash
(e)
CFTR inh-172
(f) wash
200 ms
D
nA
8
4
0
-4
-8
cpt-cAMP
+ 5ab
CFTR inh-172
200 ms
nA
6
4
2
0
-2
-4
-6
5ab
cpt-cAMP
CFTR inh-172
mV
-100
0
100

Figure 4